Journal of the European Ceramic Society **13** (1994) 221–228

Processing of Aluminium Nitride Powder by the Tape-Casting Process

M. Descamps, G. Moreau, M. Mascart & B. Thierry

CRITT Céramiques Fines, Laboratoire des Matériaux Industriels,
Université de Valenciennes et du Hainaut-Cambrésis, France

(Received 14 July 1993; revised version received 20 October 1993; accepted 10 November 1993)

Abstract

The elaboration of thin ceramic sheet requires the tape-casting process. This work, carried out on aluminium nitride, has allowed a better understanding of the different stages of the material processing by this technique. Slurry stabilization and dispersion are studied by electrical and microelectrophoretic measurements. An electrosteric stabilization model is proposed. Different binders and plasticizer types are tested for the same slurry weight formulation. The effect of these components on slurries and tapes properties is analysed and important variations of physical, mechanical, thermal and rheological characteristics are recorded. Deformation and cracking arising from the tape drying or sintering are studied and connected to powder granularity and green tape density.

Dünne Keramikplatten wurden mit Hilfe des Bandgießverfahrens hergestellt. In der vorliegenden Arbeit wurde Aluminiumnitrid untersucht, um die verschiedenen Schritte der Materialherstellung bei diesem Verfahren zu verstehen. Die Untersuchung der Stabilisierung und Dispersion des Schlickers erfolgte mit Hilfe von elektrischen und mikroelektrophoretischen Messungen. Ein elektrosterisches Stabilisierungsmodell wird vorgeschlagen. Bei gleicher Zusammensetzung des Schlickers wurden verschiedene Binder und Plastifizierungsmittel getestet. Der Effekt dieser Komponenten auf den Schlicker und die Bandeigenschaften wurden analysiert; es zeigten sich bedeutende Unterschiede in den physikalischen, mechanischen, thermischen und rheologischen Eigenschaften. Die Deformation und Rißbildung aufgrund der Bandtrocknung oder -sinterung wurden untersucht und mit der Pulverkörnung und der Grünbanddichte korreliert.

La fabrication de matériau de fine épaisseur nécessite l'utilisation du procédé par coulage en bande. Ces travaux, réalisés sur le nitrure d'aluminium ont permis d'appréhender les différentes étapes d'élaboration du produit par cette technique. La dispersion et la stabilisation des suspensions sont étudiées par des mesures de microélectrophorèse et conductivité électriques. Un modèle de stabilisation électrostérique est proposé. Différents types de liants et plastifiants sont testés, pour une même formulation pondérable de barbotines. L'influence de ces produits sur les caractéristiques des suspensions et bandes obtenues, montrent d'importantes variations des caractèristiques physiques, mécaniques, thermiques et rhéologiques. La déformation et la fissuration intervenant lors du séchage ou du frittage des bandes sont étudiées et correllées à la granularité de la poudre et à la densité des bandes à l'état cru.

1 Introduction

During recent years, aluminium nitride has gained the interest of many manufacturers as a constitutive material for substrates destined for the high power circuitry in the microelectronics field. This interest is particularly justified by a thermal conductivity notably higher than the conductivity of the widely used alumina substrates.[1,2]

The thin ceramic sheets for substrates are usually fabricated by the tape-casting process. A slurry (containing ceramic powder, a solvent system, an organic binder, one or more plasticizers, a dispersant and other additives) is cast, by means of a doctor blade, on to a mobile plastic film carrier. After drying, the green tape is then punched, sintered and finally characterized (Fig. 1).

The literature relates the wide empiricism of this process. For this reason, the different stages of the elaboration steps were studied in order to achieve their optimization.

Journal of the European Ceramic Society 0955-2219/94/$7.00

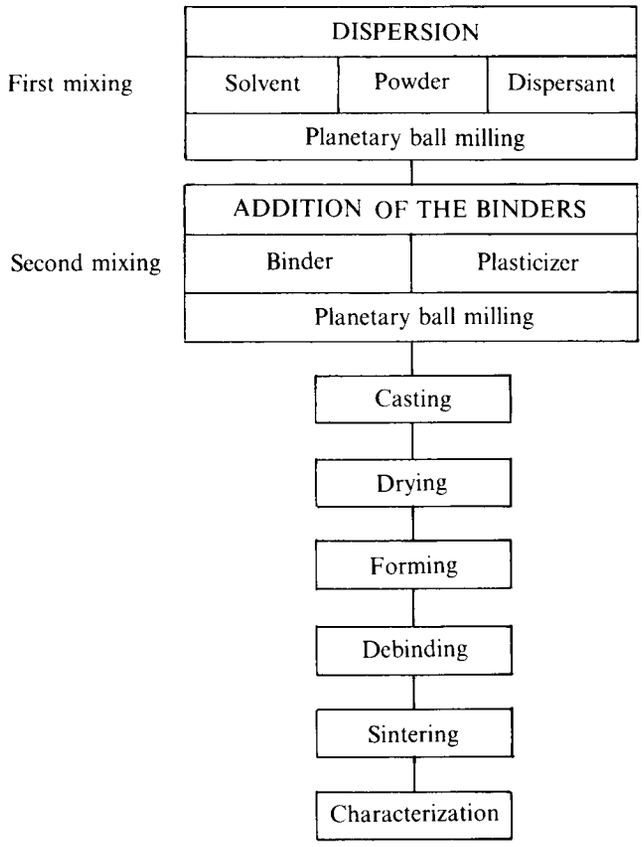

Fig. 1. Elaboration of a substrate by tape-casting.

2 Experimental Procedure

2.1 Starting material

The tape-casting of aluminium nitride was studied using different commercial raw materials (Table 1): the powders (H.C. Starck, Berlin, Germany) were synthesized by direct nitridation of aluminium. Grades A, B, C were chosen which exhibit a great diversity in mean grain sizes.

2.2 Slurry composition

AlN slurry dispersion is carried out in a binary solvent mixture of 66–34 vol.% butanone–ethanol. The selected dispersing agent belongs to the phosphate ester family (e.g. Beycostat C213, CECA, France). This dispersant is prepared by reaction between phosphoric acid and ethoxylate. The chemical structure of phosphate monoester is shown in Fig. 2. The ethoxylate is obtained by condensation of ethylene oxide in alcohol. Dry matter content is fixed to 70 wt% for all experiments.

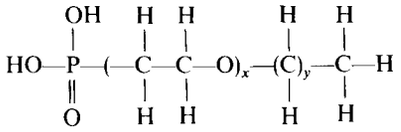

Fig. 2. Chemical structure of phosphate monoester.

Numerous experimental compositions of tape-casting slurries are reported in the literature.[3–5] A literature survey indicates that essentially two kinds of binders are used for tape-casting:

—Poly(vinylbutyral) resin (PVB) (e.g. Butvar B98, Monsanto, USA),
—Acrylic resin (AR) (e.g. Acryloïd B7, Rohm et Haas).

Poly(vinylbutyral) and acrylic resins are usually plasticized by dioctyl, dibutyl or butylbenzyl phthalates (DOP, DBP, BBP) and poly(ethylene glycol) (PEG), both of which are introduced in equal quantity in the slurry.

AlN slurries and tapes are elaborated with these constituents in order to determine their effects on the product properties. The powder used is Starck grade B, the binder content is fixed to 4·5 wt% (of AlN concentration) and the plasticizer content is equal to 125 wt% (of binder concentration).

2.3 Suspension characterization

AlN particle electrophoretic mobility in the binary solvent of 2-butanone–ethanol was measured by a Doppler electrophoretic light scattering analyser (Coulter Delsa 440). This method combines two technologies: electrophoresis, which characterizes particles by their movement in an applied electric field, and laser Doppler velocimetry, which allows measurement of the speed of particles by analysing the Doppler shifts of scattered light.

Measurements were carried out on slurries including 0·03 wt% AlN with different concentrations of phosphate ester.

Electrical conductivity measurements of 2-butanone–ethanol slurries enabled evaluation of the variations in ionic conductivity of the medium in the presence of the dispersing agent. The apparatus used is the CVD V62 (Solea Tacussel Society).

The study of rheological behaviour shows the influence of the various organic constituents on

Table 1. Physical and chemical characteristics of powders

Powder	*Chemical analysis*					*Powder mean φ (μm)*	*BET specific surface (m^2/g)*
	N (%)	*O (%)*	*C (%)*	*Fe (ppm)*	*Si (ppm)*		
Starck grade A[a]	31·5	1·5	0·10	100	—	5·2	1·2
Starck grade B[a]	32·0	2	0·10	100	—	1·7	3·7
Starck grade C[a]	29·5	2·5	0·10	100	—	1·3	4·5

[a] Hermann C Starck Berlin GmbH, Germany.

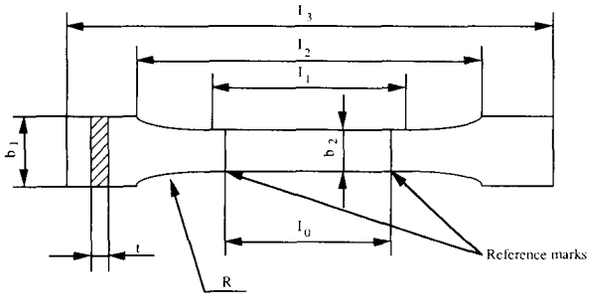

Fig. 3. Traction specimen after NFT 51034 norm. Dimensions in mm. l_3, length overall 150; b, end width, $20 \pm 0{\cdot}5$; l_1, length of calibrated part, $60 \pm 0{\cdot}5$; b_2, width of calibrated part, $10 \pm 0{\cdot}5$; R, minimal radius, 60; l_0, distance between reference marks, $50 \pm 0{\cdot}5$; l_2, initial distance between grips, $115 \pm 5{\cdot}0$, t, thickness.

slurry viscosities. Measurements are operated by means of a coaxial cylinder viscometer (TV20 Haake model). Shear stresses are recorded using shear rates up to $150\,s^{-1}$, at 20°C.

2.4 Tape characterization

Open pore diameters and densities were determined by mercury porosimetry (Poresizer 9310, Micromeritics) on green and debonded tapes elaborated with the different formulations. Samples were debonded at a temperature of 500°C, in air.

The rupture strength and elongation of green tapes were determined (Fig. 3). Measurements were performed two weeks after the slurry casting. The loading rate of the universal testing machine (Instron 1135) was fixed at 10/min/min. The standard specimen was 0·4 mm thick and ten specimens of each formulation were tested.

The thermal behaviour of the organic constituents and AlN oxidization temperature were evaluated by thermogravimetric analysis, in air (Setaram DTA92).

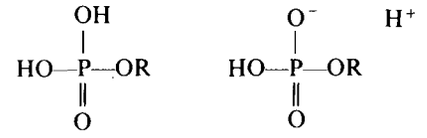

Fig. 5. Dissociation mechanism of phosphate ester.

3 Results and Discussion

3.1 Dispersion

The electrical conductivity values, recorded on the 2-butanone–ethanol–phosphate ester mixture, increase simultaneously with the increasing of dispersant concentration (Fig. 4). This fact corroborates the dissociation mechanism of phosphate ester in the tested solvent[6,7] (Fig. 5). An H^+ ion is released in the solution. The ester molecule acts as an anionic surfactant in the medium.

Electrophoretic mobility measurements show positive initial charge at the AlN powder surface in the solvent. The phosphate ester addition induces an important increasing of the powder mobility (Fig. 6). The increase, at first very important for small quantities of phosphate ester, tends to a limit for a content of 1 wt% phosphate ester/dry matter.

Recent work,[8] carried out by X-ray photoelectron spectroscopy (XPS), proposes a composition model for commercial AlN powders. In this model, an oxynitride-type phase (AlO_xN_y), would form an intermediate layer between the nitride core and the external oxyhydrated phase [AlOOH, $Al(OH)_3$] (Fig. 7).

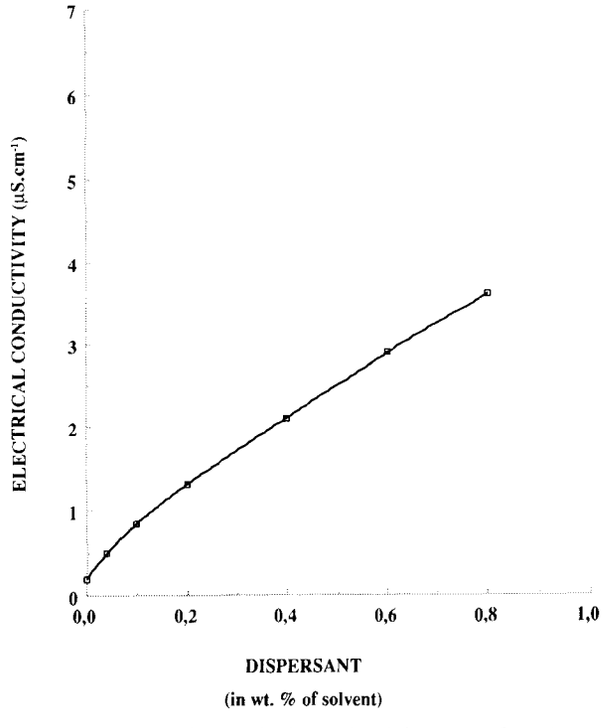

Fig. 4. Evolution of electrical conductivity as a function of dispersing agent content.

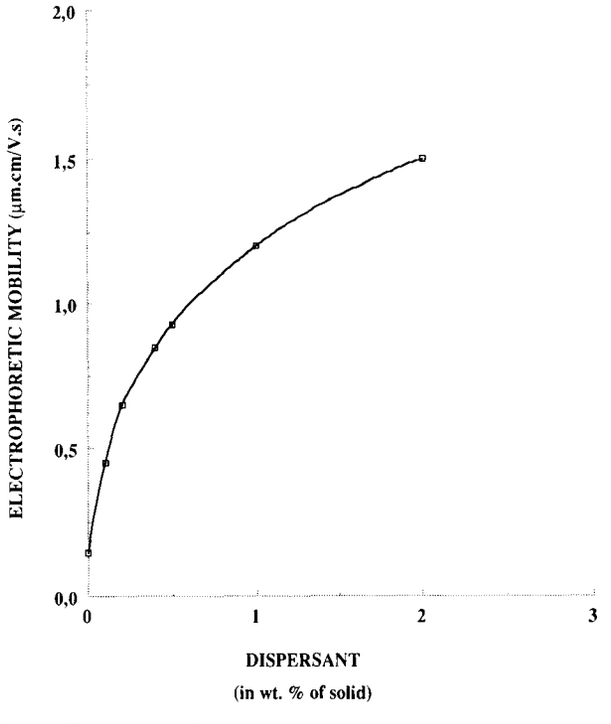

Fig. 6. Evolution of electrophoretic mobility as a function of dispersant percentage.

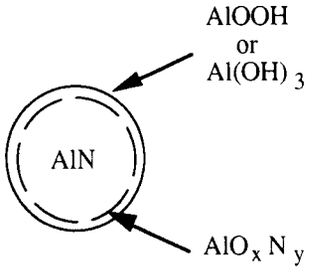

Fig. 7. Composition model of AlN grains (Ref. 8).

The increasing positive charge of the AlN powder can be explained by an interaction between amphoteric OH groups present at the AlN surface, and H^+ ions released by the dispersing agent, following the acid–base reaction:

$$AlOOH + H^+ \rightleftharpoons AlOOH_2^+$$

The ester ionization induces a higher positive charge at the particle surface, due to the adsorption of H^+ ions. The anionic end of phosphate ester is attracted to the positively charged surface of AlN by coulombic forces. The nonpolar hydrocarbon tail extends into the organic solvent.

The suspension is electrosterically stabilized. Indeed, electrostatic repulsion effects due to particle electric charge are combined with steric repulsion effects ensured by the polymeric chains of dispersant. The efficiency of this surfactant is then evaluated by means of viscosity measurements of planetary ball-milled AlN slurries. This experimentation is carried out on suspensions with different dry matter contents: 65, 70, 75, 80 wt% (Fig. 8). Results show that small quantities of phosphate ester lead to very low viscosity: 30 mPa s for 80 wt% AlN in 2-butanone–ethanol and with 0·6 wt% (of AlN content) phosphate ester, a shear rate of 25 s^{-1}. The efficiency of this dispersing agent is confirmed by granulometric and sedimentation tests.

3.2 Binder and plasticizer

After the dispersion step, other organic constituents (binders and plasticizers) are added to the slurry. These products confer strength to the green tape.

Slurries are formulated with the main binders commonly used for tape-casting: poly(vinylbutyral) and acrylic resin (4·5 wt% of AlN content). Plasticization trials are carried out for these resins with dioctyl, dibutyl and butylbenzyl phthalates (DOP, DBP, BBP), poly(ethylene glycol) (PEG 400) (125 wt% of binder content) and mixing of these plasticizers, in equal quantities in the slurry.

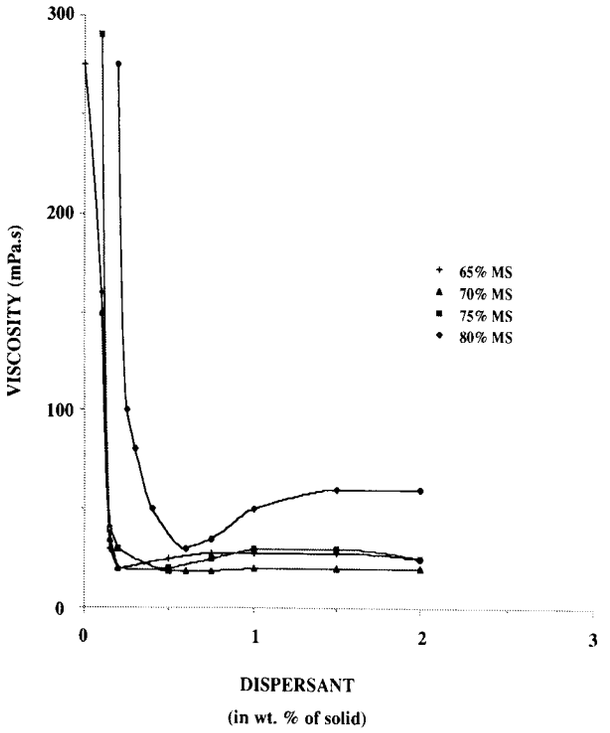

Fig. 8. Evolution of viscosity as a function of dispersant percentage (shear rate = 25 s^{-1}).

Rheological, mechanical and physical properties of slurries and tapes as well as the thermal behaviour of organic constituents are determined in order to show their effects on the cast tape.

3.2.1 Rheological properties

The viscosities of the slurries containing PVB are higher than those containing acrylic resin (Table 2). For a fixed resin, weak slurry viscosity variations are recorded for the different phthalates. However, the poly(ethylene glycol) induces an increase of slurry viscosity.

3.2.2 Mechanical properties

Ultimate tensile strength of green tapes elaborated with acrylic resin is little affected by the chemical nature of the plasticizer. The highest rupture deformation is obtained with the dioctyl phthalate

Table 2. Viscosity (mPas) of different suspensions (shear rate 100 s^{-1})

Resin[a]	*Plasticizers*[a]						
	DOP	*DBP*	*BBP*	*PEG*	*DOP + PEG*	*DBP + PEG*	*BBP + PEG*
PVB	1 096	1 127	1 191	1 417	1 209	1 277	1 412
AR	574	471	544	690	579	596	760

[a] DOP, Dioctylphthalate; DBP, dibutyl phthalate; BBP, butylbenzyl phthalate; PEG, poly(ethylene glycol); PVB, poly(vinylbutyral) resin; AR, acrylic resin.

Table 3. Mechanical properties of green tapes with acrylic resin

	Plasticizers						
	DOP	*DBP*	*BBP*	*PEG*	*DOP + PEG*	*DBP + PEG*	*BBP + PEG*
Rupture strength (MPa)	0·34	0·30	0·37	2·55	0·39	0·31	0·38
Rupture deformation (%)	17·5	3·2	5·5	0·3	12·5	5·9	11·6

Table 4. Mechanical properties of green tapes with polyvinylbutyral

	Plasticizers						
	DOP	*DBP*	*BBP*	*PEG*	*DOP + PEG*	*DBP + PEG*	*BBP + PEG*
Rupture strength (MPa)	1·35	1·1	1·42	1·8	0·92	0·54	0·58
Rupture deformation (%)	4·8	10·5	8·8	2	8·5	10·9	11·4

Table 5. Open porosity diameter of green and debinded tapes and density of debinded tapes with acrylic resin

	Plasticizers						
	DOP	*DBP*	*BBP*	*PEG*	*DOP + PEG*	*DBP + PEG*	*BBP + PEG*
ϕ mean pore diameter of green tapes (μm)	0·43	0·44	0·44	0·43	0·43	0·45	0·44
ϕ mean pore diameter of debinded tapes (μm)	0·33	0·34	0·33	0·34	0·33	0·33	0·34
Relative density of debinded tapes (%)	61·8	61·9	62·5	61·3	61·7	61·2	62

Table 6. Open porosity diameter of green and debinded tapes and density of debinded tapes with polyvinylbutyral

	Plasticizers						
	DOP	*DBP*	*BBP*	*PEG*	*DOP + PEG*	*DBP + PEG*	*BBP + PEG*
ϕ mean pore diameter of green tapes (μm)	0·45	0·44	0·45	0·43	0·43	0·44	0·43
ϕ mean pore diameter of debinded tapes (μm)	0·34	0·35	0·35	0·34	0·35	0·35	0·36
Relative density of debinded tapes (%)	59·5	59·5	59·9	59·9	59·8	59·9	59·3

(17·5%) and the lowest with the polyethylene glycol (0·3%) (Table 3).

With poly(vinylbutyral), the ultimate tensile strength varies on a large scale according to the plasticizer introduced in the tape. This strength is maximal with butylbenzyl phthalate and poly(ethylene glycol) and decrease highly when a plasticizer mixture is used. The dibutyl phthalate and the butylbenzyl phthalate–poly(ethylene glycol) mixture result in the highest elongations (Table 4). The comparative study of these results shows that, for the same weight formulation, the best stress is obtained for poly(vinylbutyral) with butylbenzyl phthalate, but deformation is maximal for acrylic resin with dioctyl phthalate. Finally, the single poly(ethylene glycol) shows a weak effect on tape plasticization for both resins.

3.2.3 Physical properties

For the two resins, the plasticizer type has little effect on tape physical characteristics (Tables 5 and 6). Indeed, the open pore mean diameters of green and debonded tapes are equal to $0{\cdot}44\,\mu m \pm 0{\cdot}01$ (PVB) and $0{\cdot}34\,\mu m \pm 0{\cdot}01$ (AR). The relative density of PVB debinded tapes is close to 60%, whereas the relative density of debinded tape elaborated with acrylic resin is close to 62%, whatever plasticizer has been used.

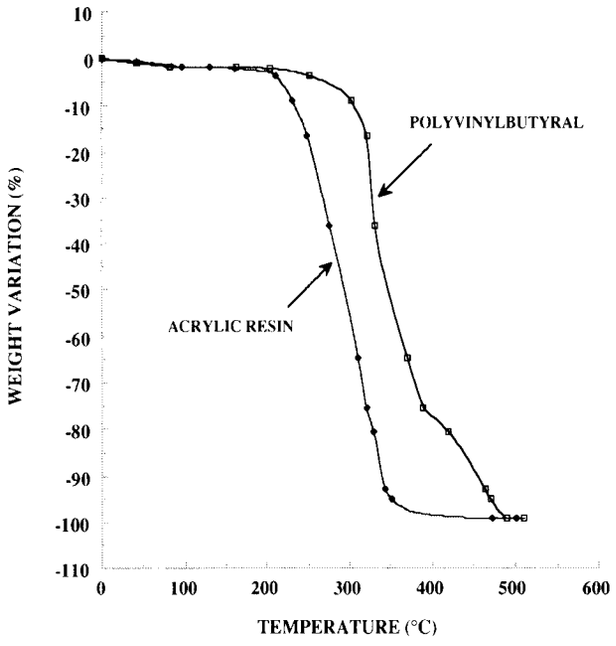

Fig. 9. PVB and AR removal.

However, the comparison of experimental results reveals higher densities for AR debonded tapes (two percent), than for PVB debinded tapes. The acrylic organic phase offers a weak resistance to particle movement, which improves the sliding between those particles and leads to a maximal packing of powder grains. On the other hand, a high evaporation rate of organic solvents involves a fast increase of the cast tape viscosity and structure 'freezing'. Thus, a low slurry viscosity will allow an easier and faster powder packing.

3.2.4 Thermal properties

The thermal behaviour of organic components was determined by thermogravimetric analysis (TGA)

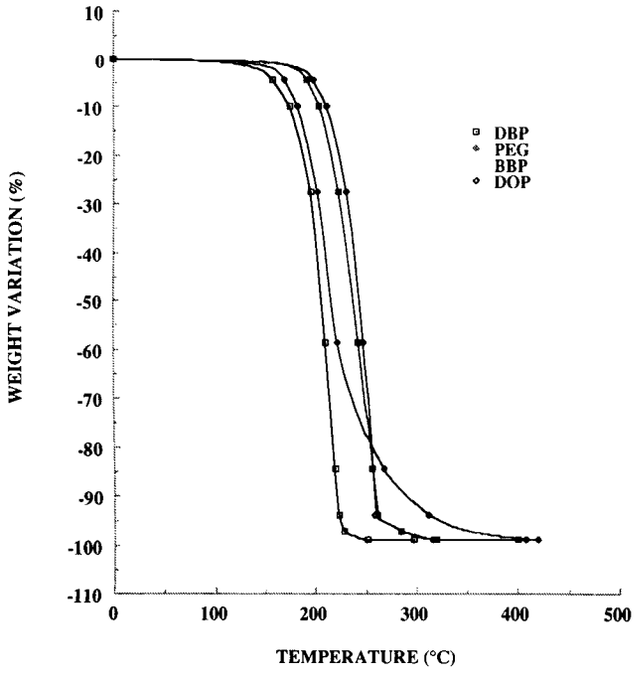

Fig. 10. BBP, DOP, DBP, PEG removal.

(Figs 9 and 10). The thermal treatment was under air with a heating rate of 1°C/min. The poly(vinylbutyral) and acrylic resin removal end respectively at 490°C and 410°C. The poly(vinyl alcohol) present in the PVB (20 wt%) induces the anomaly observed on the curve (400°C) and involves a more difficult thermal degradation compared to the acrylic resin.

Phthalates (DBP, DOP, BBP) show a total and easy elimination to low temperatures. Evaporation rates of these products are fast because their molecular weights are low. The PEG is completely burned out at a higher temperature (420°C), due to the polymer degradation before its elimination.

For AlN powder, the debonding atmosphere is extremely crucial. Indeed this material is particularly sensitive to oxygen and is converted Al_2O_3 at high temperature.[9,10] The temperature at which AlN oxidation begins must be studied in order to determine if debonding of organic components in an oxidizing atmosphere is possible without formation of Al_2O_3. The following experimentation is performed using thermogravimetric analysis (TGA).

The change of AlN to Al_2O_3 is accompanied by an important weight variation. The oxidation temperature is determined by TGA by two methods. At first, AlN powder is heated to 1400°C at a slow rate (0·5°C/min). Weight begins to increase at 660°C. The change of AlN to Al_2O_3 is complete at 1100°C. The oxidation seemed therefore to start at 660°C. To refine this measurement and evaluate the influence of time, AlN isothermal treatments are carried out at various temperatures from 500°C to 900°C.

The treatment dwell time was 2 h. No increase in weight was observed for powder heated at 500°C and 600°C. Furthermore, a slight variation is recorded at 650°C. This increase becomes more sensitive with increasing temperature. Complementary experiments showed that a dwell time of 20 h at 600°C involved no weight variation of AlN and weight increases of 0·12% for the same thermal treatment at 650°C. As a conclusion, organics which achieve decomposition below 500°C can be burnt under oxidizing atmosphere (air) up to 600°C without AlN alteration,

3.2.5 Conclusion

The whole of these experimental results have oriented the binder choice toward acrylic resin. Indeed, this component gives viscosities lower than PVB suspensions, and allows an increase in the dry matter content in slurries. Thus, after qualitative and quantitative optimization of organic constituents, slurries with 75 wt% of AlN are elaborated.

In addition, acrylic resin is removed at a lower temperature than PVB and leads to increase the green tape density. The lowest values of strength

observed for AlN tapes elaborated with acrylic resin are adequate for handling and storing.

Concerning plasticizers, results show the weak plasticization power of PEG for these two resins. Moreover, this component exhibits a high debonding temperature, induces increases in the slurry viscosity and has hygroscopic properties. For these reasons, PEG is prohibited from casting slurry elaboration.

Acrylic resin is plasticized by DOP and BBP. These products confer correct tape characteristics and are compatible with post-casting operations.

3.3 Drying

The AlN slurries are cast on a tape-casting bench by the doctor blade method. The casting of AlN tape presents, for some powders, a lot of difficulties, especially when thick tapes are needed. Warping and numerous cracks may appear during drying. Many studies, and particularly those carried out by Scherer and coworker[11,12] in the sol–gel field, showed that the capillary tension generated by the open porosity of the material is a possible source of damage for these materials.

3.3.1 Capillary pressure

The amplitude of the capillary tensions generated within the tape is directly related to the mean diameter of the open pores. During drying, the amount of solvent decreases and the liquid–vapour interface becomes curved, with a radius of curvature r, so that the free energy of the system can be minimized. The formation of the meniscus produces a tension in the liquid equal to:

$$P_r = -2\gamma_{LV}/r$$

where γ_{LV} is the liquid–vapour interfacial energy. This capillary tension increases when the radius of the meniscus falls.

The tension induces compressive stresses on the solid phase which force it to contract. However, a large pressure gradient ($\vec{\nabla}P$) develops within the porous body so that the material is more compressed near the external surface than in the core. The strong capillary tensions and the differential shrinkage may cause drying stresses which are likely to damage the material.[7]

With the aim of relating the mean diameter of open pores to cracking, tapes are elaborated with different grades of AlN powders (Table 7). This experimental approach enabled green tapes with various mean pore diameters to be obtained. Numerous cracks are visually detected on the tapes prepared from slurries which contained Starck grade C powder. The mean pore diameter recorded for this powder is 0·28 μm. The tapes prepared from Starck grade B powders show a lower degree of cracking. Tape containing Starck grade A is free of defects and has a pore diameter of 1·47 μm. The experimental data illustrate the strong propensity of tapes to crack when the mean pore diameter decreases. High capillary tensions are generated by these small pore diameters. The effect of these tensions in the damaging of material is therefore confirmed.

Table 7. Surface aspects and open pore mean diameters

Powder	*Grain size* (μm)	*Surface aspect*	*Mean porosity diameter* (μm)
Starck grade A	5·2	No cracks	1·47
Starck grade C	1·3	Cracked	0·28

With a view to corroborate these results, tapes are cast with mixtures of AlN powders. These mixtures are composed of Starck AlN powder grade A and Starck powder grade C. Grade A possess a mean particle size of 5·2 μm. In contrast, the granulometry of the grade C is finer (mean particle size 1·3 μm). With this procedure, an increase of the mean diameter of the tape open porosity is obtained (Fig. 11).

As a result, no cracks are visually detected on the surface of tapes composed of a mixture of Starck powders: 50% grade A + 50% grade C (corresponding mean pore diameter: 0·42 μm). These facts have confirmed the previous experimentation made on Starck grade A powder.

An increasing mean pore diameter reduces capillary pressures and, in this way, eliminates tape cracking. In the frame of this work, it is found that a mean diameter of about 0·40 μm avoids cracking.

Furthermore, porosimetry measurements performed on green tapes demonstrate the tape density

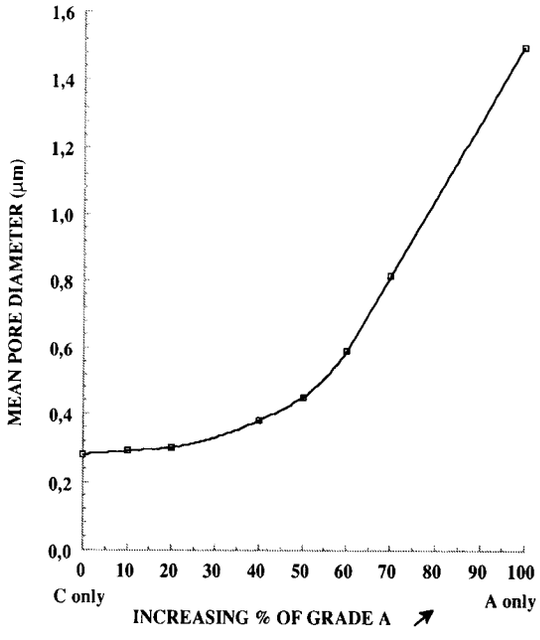

Fig. 11. Evolution of tape mean pore diameter as a function of the ratio of AlN grade A versus AlN grade C.

heterogeneity. Indeed, trials realized on tapes for which one face was made mercury-tight, reveal an important difference of pore mean diameters between superior and inferior faces of the tape. This experimentation was carried out by mean the sticking of thin glass sheet on each face of the green tape. The face in contact with the mobile carrier (plastic film) shows a larger diameter (0·43 μm) than the one measured on the face where the solvent evaporates (0·34 μm). The pressure gradient ∇P developed by the porous material, the viscosity increasing during the drying and interactions between plastic film and tape are all factors which contribute to this phenomenon.

The density heterogeneity between tape bottom and top can induce a differential shrinkage and cause distortion often encountered during the substrate sintering.[13,14]

4 Conclusions

The experimental study carried out on elaboration stages of AlN sheets obtained by the tape-casting technique has led to:

—The proposition of an electrosteric stabilization model of AlN powders in the 2-butanone–ethanol–phosphate ester medium. Electrophoretic measurements show an increase of AlN positive charge with dispersant. The positive charge allows the surfactant to anchor on the powder surface by electrostatic attraction.

—Identification of the effects of organic constituents (binders, plasticizers) on thermal, mechanical, physical and rheological properties of AlN tapes and slurries. The quantitative optimization of these polymeric components will depend on the post-casting operations and the final material applications.

—The evaluation of the powder granularity influence, and therefore the open porosity diameter of tape, on the green tape cracking.

—Demonstration of the presence of a powder compaction gradient inside the tape. This density variation can explain distortion during the material sintering.

Acknowledgement

The authors thank the European Community (EEC) for providing funds in the frame of a BRITE-EURAM program, Contract No. BREU-0055-C.

References

1. Kuramoto, N., Taniguchi, H. & Aso, A., Development of translucent aluminium nitride ceramics. *Am. Ceram. Soc. Bull.*, **68** (1989) 883–7.
2. Sheppard, L. M., Aluminium nitride: a versatile but challenging material. *Am. Ceram. Soc. Bull.*, **69** (1990) 1801–12.
3. Moreno, R., The role of slip additives in tape-casting technology. *Am. Ceram. Soc. Bull.*, **71** (1992) 1647–57.
4. Mistler, R. E., Tape-casting: the basic process for meeting the needs of electronics industry. *Am. Ceram. Soc. Bull.*, **69** (1990) 1022–6.
5. Mistler, R. E., Shanefield, D. J. & Runk, R. B., Tape-casting of ceramic. In *Ceramic Processing Before Firing*, ed. G. Y. Onoda & L. L. Hench. Wiley, NY, 1976, pp. 411–48.
6. Cannon, W. R., Morris, J. R. & Mikeska, K. R., Dispersants for nonaqueous tape-casting. In *Advances in Ceramics*, Vol. 19, ed. J. B. Blum & W. T. Cannon. American Ceramic Society, Westerville, OH, 1986, pp. 161–74.
7. Morris, J. R., Organic component interactions in tape-casting slips of barium titanate. PhD thesis, Rutgers University, New Jersey, 1986.
8. Ponthieu, E., Grange, P., Delmon, P., Lonnoy, L., Leclercq, L., Bechara, R. & Grimblot, J., Proposal of a composition model for commercial AlN powders. *J. Eur. Ceram. Soc.*, **8** (1991) 233–41.
9. Katnani, A. D. & Papathomas, K. I., Kinetics and initial stages of oxydation of aluminium nitride: thermogravimetric analysis and X-ray photoelectron spectroscopy study. *J. Vac. Sci. Technol. A*, **5** (1987) 1335–40.
10. Suryanarayana, D., Oxidation kinetics of aluminium nitride. *J. Am. Ceram. Soc.*, **73** (1990) 1108–10.
11. Scherer, G. W., Theory of drying. *J. Am. Ceram. Soc.*, **73** (1990) 3–14.
12. Brinker, C. J. & Scherer, G. W., *Sol–Gel Science, the Physics and Chemistry of Sol–Gel Processing*. Academic Press, NY, 1990, pp. 453–513.
13. Williams, J. C., In *Treatise on material science and technology*, ed. F. F. Wang. Academic Press, NY, 1976, pp. 173–98.
14. Wilkinson, D. S., Plucknett, K. P. & Caceres, C. H., Tape-casting using fine ceramic powders. *Mat. Res. Soc. Symp. Proc.*, **249** (1992) 305–10.